Journal of Drug Delivery Science and Technology 114 (2025) 107498

Contents lists available at ScienceDirect

Journal of Drug Delivery Science and Technology

journal homepage: www.elsevier.com/locate/jddst

Liposomal sprays for nasal vaccination: a comparative study of cationic and anionic formulations involving stability upon nebulization, sprayability, and *in vitro* immune activation

Matteo Aroffu [a,c], Federica Fulgheri [a], Rita Abi Rached [a], Ines Castangia [a], Annunziata Corteggio [b], Paola Italiani [b], Luciana D'Apice [b], Myriam Sainz-Ramos [c,d,e,f], Fátima García-Villén [g], Xavier Fernàndez-Busquets [h,i], Maria Manconi [a,*], José Luis Pedraz [c,d,e,f], Maria Letizia Manca [a], Anna Maria Fadda [a]

[a] Department of Life and Environmental Sciences, University of Cagliari, University Campus, S.P. Monserrato-Sestu Km 0.700, 09042, Monserrato, (CA), Italy
[b] Institute of Biochemistry and Cell Biology, National Research Council, Via Pietro Castellino 111, 80131 Napoli, Italy
[c] NanoBioCel Research Group, Faculty of Pharmacy, University of the Basque Country (UPV/EHU), Paseo de La Universidad 7, 01006, Vitoria-Gasteiz, Spain
[d] Biomedical Research Center in Bioengineering, Biomaterials and Nanomedicine (CIBER-BBN), 01006, Vitoria-Gasteiz, Spain
[e] BioAraba, NanoBioCel Research Group, Calle Jose Atxotegi, S/n, 01009, Vitoria-Gasteiz, Spain
[f] Joint Research Laboratory (JRL), School of Pharmacy, University of the Basque Country (UPV/EHU), 01006, Vitoria-Gasteiz, Spain
[g] Department of Pharmacy and Pharmaceutical Technology, School of Pharmacy, University of Granada, Campus of Cartuja, 18071, Granada, Spain
[h] Barcelona Institute for Global Health (ISGlobal, Hospital Clínic-Universitat de Barcelona), Rosselló 149-153, ES-08036, Barcelona, Spain
[i] Nanomalaria Group, Institute for Bioengineering of Catalonia (IBEC), The Barcelona Institute of Science and Technology, Baldiri Reixac 10-12, ES-08028, Barcelona, Spain

ARTICLE INFO

Keywords:
Liposomes
Nanovaccines
Nasal drug delivery
Spray
Ovalbumin
Alberta idealized nasal inlet

ABSTRACT

Nasal immunization is a promising non-invasive route, enabling needle-free self-administration and activating immune cells in the mucosal tissue of the upper airways. This vaccination method is particularly appealing when paired with biocompatible and biodegradable nanocarriers like liposomes, which serve as an effective tool for the nasal delivery of antigenic molecules. In the present study, the model antigen ovalbumin was encapsulated in liposomes using an eco-friendly method. Negative and positive liposomes were formulated with Phospholipon® 90 G alone (anionic liposomes) or combined with 1,2-dioleoyl-3-trimethylammonium-propane (cationic DOTAP-liposomes). These liposomes were smaller than 130 nm and remained stable for up to 3 months. Their sprayability was assessed based on criteria established by the European Medicines Agency and the Food and Drug Administration for nasal products. Both formulations were easily sprayable, generating droplets larger than 5 μm, which are expected to deposit in the nose while avoiding the lungs. Furthermore, after nebulization, they retained their dimensions, structures, and high encapsulation efficiencies (>70 %). In a co-culture system of dendritic cells and B3Z OT-I hybridoma cells, it was shown that they enhanced antigen delivery and presentation, producing approximately 6–9 times more interleukin-2 compared to the ovalbumin solution. Lastly, when tested on macrophages, they did not induce any proinflammatory effect. However, due to their higher mucoadhesiveness (~88 % vs ~8 %) and better deposition in the posterior nasal cavity (~52 % vs ~43 %) compared to anionic liposomes, cationic DOTAP-liposomes appeared more suitable for nasal administration.

1. Introduction

Vaccination has evolved since its discovery in 1798, adapting to the changing needs and concerns of users [1–3]. Although some people remain unconvinced about the usefulness of vaccination, most of the population appears to recognize its importance and trusts that new technologies will enable simpler, less painful, and more user-friendly methods of administration [4,5]. Currently, most vaccines are

This article is part of a special issue entitled: Skin and mucosal drug delivery published in Journal of Drug Delivery Science and Technology.

* Corresponding author.
E-mail address: manconi@unica.it (M. Manconi).

https://doi.org/10.1016/j.jddst.2025.107498
Received 17 July 2025; Received in revised form 4 September 2025; Accepted 6 September 2025
Available online 6 September 2025

administered parenterally, intramuscularly, or subcutaneously, with several consequent problems that include inconvenience, local pain, need for professional assistance, and high expenses. To address these issues, several non-invasive administration routes (i.e., oral, transdermal, nasal, and pulmonary) have been exploited over the last decades [6–10]. Among all, the nasal route, typically harnessed by many pathogens for infection, is a convenient site for drug delivery and immunization and represents a reliable and patient-friendly alternative to the parenteral or even oral route [11–14]. Indeed, the nasal mucosa itself offers a wide range of advantages, starting from its easy and manageable access and the presence of a relevant network of immune cells known as nasopharyngeal-associated lymphoid tissue (NALT). Therefore, the ability to stimulate the immune system at this level can provide localized protection against pathogens, enable their rapid clearance, promote the induction of long-term immunity through central and tissue-resident memory cells, and offer new capabilities to regulate the responses [15]. Due to the anatomy of the mucosa, characterized by low thickness and high vascularisation, the nasal route possesses the additional benefit of being suitable not only for local but also for systemic responses, allowing bypass of the hepatic first-pass metabolism. However, even though the enzymatic activity in loco is poor compared to the hepatic first-pass metabolism, it must be taken into account when it comes to proteins or antigens, as in the case of vaccines, due to the presence of proteases [16]. An effective way to protect antigens from degradation is represented by nanocarriers such as liposomes, vesicles with a small size (<1000 nm) capable of including the antigen in their structure, which basically consists of an internal aqueous reservoir surrounded by a lipidic bilayer [17–19]. This peculiar assembling, along with their safety, optimal performances in targeted delivery, and composition-dependent adjuvanticity, has prompted scientists worldwide to develop intranasal vaccines with liposomes [20,21]. Some researchers have evaluated these liposomal formulations against various airborne pathogens, including SARS-CoV-2, *Yersinia pestis*, and Group A *Streptococcus*, as well as lung cancers [22–27]. Others have utilized liposomes loaded with model antigens like ovalbumin to explore the mechanisms beyond the associated immune responses [28–32]. Despite the remarkable achievements in immune response, important elements such as 1) the use of potentially harmful solvents or materials during vesicle preparation, 2) the significance of the surface charge for the intranasal route, and 3) the impact of the nebulization process on the integrity of the liposomes are often overlooked.

In this study, the model antigen ovalbumin was encapsulated in anionic and cationic liposomes. Notably, direct sonication was used as an organic solvent-free and reliable method to prepare phospholipid vesicles tailored for nasal immunization [33]. A mixture of phosphatidylcholines was used as the main lipidic component due to their safety and absorption-enhancing properties [34]. Dioleoyl-3-trimethylammonium propane (DOTAP) was chosen to impart a positive charge to the liposomes and improve the interaction with mucus and immune cells [35]. The physicochemical properties of vesicles were assessed and compared before and after nebulization using a commercial spray device (Nasonex®). A comprehensive analysis of the nasal spray containing the loaded vesicles was conducted, utilizing laser diffraction and the cutting-edge Alberta Idealized Nasal Inlet (AINI) replica, which is representative of a wide range of patient anatomies. This allowed for the determination of the size distribution of the generated droplets and the evaluation of their regional deposition patterns [36]. Lastly, the antigen presentation and inflammatory response were evaluated after exposing murine bone marrow-derived dendritic cells and human monocyte-derived macrophages to the ovalbumin-encapsulated liposomes [33].

2. Materials and methods

2.1. Materials

Phospholipon® 90G (P90G, soybean phosphatidylcholine ≥94 %, lysophosphatidylcholine ≤4 %, D,L-α-tocopherol palmitate ≤0.3 %, and ascorbyl palmitate ≤0.1 %) was purchased from AVG srl (Milan, Italy). Novagen® bicinchoninic acid protein assay kit (BCA protein assay kit), Corning® syringe filters (cellulose triacetate membrane, surfactant-free, diam. 28 mm, pore size 0.2 μm), ovalbumin (Grade VI, ≥98 %), DOTAP (chloride salt), cholesterol, fluorescein isothiocyanate-dextran (FITC-dextran, molecular weight 70 kDa), lipopolysaccharide from *E. coli* O55:B5, trypan blue, and all the other reagents of analytical grade were purchased from Sigma-Aldrich (Milan, Italy). Blue patent dye and red ponceau dye were purchased from Galeno srl (Carmignano, Italy). Vivaspin® 2 centrifugal concentrators (cellulose triacetate membrane, molecular weight cut-off 100 kDa) were purchased from Thermo Fisher Scientific Inc. (Waltham, USA). Ultrapure bidistilled water was obtained from a Milli-Q R4 system, Millipore (Milan, Italy).

2.2. Preparation of liposomes

Anionic liposomes were prepared, dispersing P90G (69 mg mL^{-1}) and cholesterol (1 mg mL^{-1}) in sterile bidistilled water. To maintain a constant total lipid concentration of 70 mg mL^{-1}, cationic DOTAP-liposomes were prepared using 60 mg mL^{-1} of P90G, 9 mg mL^{-1} of DOTAP, and 1 mg mL^{-1} of cholesterol. In both cases, ovalbumin was dispersed along with the lipids at a final concentration of 5 mg mL^{-1}. Dispersions were directly sonicated twice (4 s On, 2 s Off, 5 cycles, 14 μm amplitude) using a probe sonicator Soniprep 150 (MSE Crowley, London, UK), allowing each sample to cool down for 5 min between the two sonication sessions to avoid overheating. The unencapsulated ovalbumin was subsequently removed using Vivaspin® 2 centrifuge concentrators according to section 2.2.4. Lastly, the samples (n = 3 per type) were filtered through Corning® syringe filters (pore size 0.2 μm) inside previously autoclaved vials under a laminar flow hood to obtain sterile formulations. All the vesicles were stored at 4 °C under vacuum.

2.3. Characterization of liposomes

2.3.1. Morphological features

Vesicle morphology was observed by cryogenic transmission electron microscopy (cryo-TEM) using a TECNAI G2 20 TWIN microscope (FEI, Eindhoven, The Netherlands) to evaluate their shape, lamellarity, and successful manufacture. The analysis was carried out at 200 KeV voltage in a bright-field and low-dose image mode [37]. The diluted sample dispersion (3 μL) was placed over glow-discharged 300 mesh Quantifoil TEM grids frozen, which were then plunged into liquid ethane employing a FEI Vitrobot Mark IV. The frozen grids were kept below −170 °C (liquid nitrogen temperature) in a 626 DH Single Tilt Cryo-Holder (Gatan, France) before and during cryo-TEM analysis.

2.3.2. Physicochemical characteristics

The mean diameter (MD), polydispersity index (PDI), and zeta potential (ZP) of the vesicles (n = 3 per type) were measured using a Zetasizer Ultra (Malvern Instruments, Worcestershire, UK). The MD and PDI were determined through the dynamic light scattering technique, which measures the Brownian motion of the particles in the sample. ZP was instead detected through the mixed-mode measurement-phase analysis, which measures the electrophoretic mobility of the particles in dispersion [38]. All the samples were properly diluted with water (1:100 v/v) before analysis to obtain an adequate count rate and ensure the reproducibility of the experimental measurements. The most suitable dilution to perform the analysis was chosen according to the feedback provided by the intelligent data quality advice of the ZX software (Malvern Instruments, Worcestershire, UK). The scattering angle used was 175° (back-scatter).

2.3.3. Long-term stability

All the vesicles (n = 3 per type) were stored at 4 °C and kept under vacuum before and after every measurement to prevent any cross-

contamination. MD, PDI, and ZP were measured with the Zetasizer Ultra after 1 month and 3 months of storage. Prior to analysis, samples were allowed to equilibrate at room temperature (25 °C) for 15 min and then measured at the same temperature. Each opening was performed under aseptic conditions to preserve the sterility of the content.

2.3.4. Encapsulation efficiency

EE (%) of ovalbumin within the liposomes was determined indirectly using Vivaspin® 2 centrifugal separators with a cellulose triacetate membrane. This membrane was selected over others due to its low binding affinity for macromolecules like proteins and its ability to provide the highest filtrate [39]. All the separators were pre-treated overnight with a passivation solution (Triton X, 5 % w/v) and rinsed with distilled water several times before use, according to the manufacturer's recommendations. Both vesicle dispersions were diluted with water to 7 mg mL^{-1} of total lipids and 0.5 mg mL^{-1} of ovalbumin, loaded (1 mL) into the Vivaspin® 2 centrifugal separators, and centrifuged at 1000 rpm for 2 h at 25 °C, with a centrifuge equipped with swing bucket rotor (Eppendorf Centrifuge 5804, Sigma, Italy). The amount of free ovalbumin collected in the purification filtrates was determined using the BCA protein assay kit (Novagen®, Sigma, Italy), analyzing the absorbance at 562 nm with a UV spectrophotometer (Lambda 25, PerkinElmer, Milan, Italy) [40]. All experiments were performed in triplicate. The EE (%) was calculated according to the following formula:

$$EE\ (\%) = \frac{Total\ ovalbumin - ovalbumin\ in\ the\ purification\ filtrate}{Total\ ovalbumin} \times 100\% \quad \text{(Eq. 1)}$$

2.3.5. Mucoadhesiveness

The ZP variations and mucin adsorption onto vesicle surfaces were measured to assess their muco-adhesiveness [41]. Vesicles were therefore diluted (1:80 v/v) with a mucin solution (0.5 mg mL^{-1}), vortexed for 10 s, and incubated at 37 °C for 20 min, which corresponds to the mucociliary clearance time in the nose [42,43]. ZP was measured at 37 °C every 5 min during the 20-min incubation period (0, 5, 10, 15, and 20 min) and compared with the ZP of the corresponding vesicles diluted with water. To assay the mucin adsorption, the method developed by Salade and co-workers was employed with some modifications [42]. Briefly, once the incubation time had elapsed, the vesicle dispersions diluted with mucin were centrifuged at 4000 rpm for 10 min, and 25 μL of supernatant were collected to quantify the amount of free mucin by the BCA protein assay kit (Novagen®, Sigma, Italy) [44]. To exclude any possible interaction due to lipids or ovalbumin in the quantification of mucin, empty vesicles and ovalbumin-loaded vesicles diluted with water rather than mucin were used as references. All the experiments were performed in triplicate. The percentage of mucin adsorbed onto the vesicles was indirectly calculated according to the following formula:

$$Adsorbed\ mucin\ (\%) = \frac{Total\ mucin - free\ mucin}{Total\ mucin} \times 100\% \quad \text{(Eq. 2)}$$

2.4. Sprayability of liposomes

2.4.1. Stability following nebulization

Ovalbumin-encapsulated anionic liposomes and cationic DOTAP-liposomes (6 mL) were loaded into the commercial Nasonex® device (Merck Sharp & Dohme Corp., Heist-op-den-Berg, Belgium) and completely discharged into a conical flask. The device and the conical flask were oriented at 45° to simulate the conditions required for performing the droplet size distribution and deposition studies described in sections 2.4.2 and 2.4.3, respectively. After being discharged, the vesicles were recovered and properly diluted with water to assess the MD, PDI, ZP, and EE of the sprayed vesicles. These analyses followed the same procedures and settings described in sections 2.3.2 and 2.3.4.

2.4.2. Mean droplet size and size distribution

The droplet size distribution was measured by laser diffraction using the Spraytec® (Malvern Panalytical Ltd., Malvern, United Kingdon), which detects droplets sized from 0.1 to 2000 μm. Tests were carried out at nozzle tip-to-laser distances of 4 and 7 cm, complying with the measurement range (3–7 cm) and the distance between measurements (3 cm) set by the Food and Drug Administration (FDA). Each formulation (6 mL) was transferred to the Nasonex® device. All the measurements were performed in triplicate at 25 °C, positioning the device at a 45° angle to the reading laser beam. After every actuation, the values D10, D50, and D90, which represent the respective percentage (10 %, 50 %, and 90 %) of all the particles below the registered size, along with the Span, which expresses the uniformity of the droplet size distribution, were measured.

2.4.3. Droplet deposition in the Alberta Idealized Nasal Inlet

FITC-dextran with comparable molecular weight to ovalbumin was added as a fluorescent probe to anionic liposomes and cationic DOTAP-liposomes during preparation. The Alberta Idealized Nasal Inlet (Copley Scientific, Nottingham, United Kingdom) was coated with the mucin solution (0.5 mg mL^{-1}) used in section 2.3.5 and further connected to the Next Generation Impactor (NGI) (Copley Scientific, Nottingham, United Kingdom) and a pump. The device mentioned above was filled with 6 mL of dispersions of negative or cationic DOTAP-liposomes, oriented at 45° to the Alberta Idealized Nasal Inlet, and manually actuated three times for each formulation after priming. A Petri dish was placed under the device to recover the sample in case of dripping. A steady flow rate of 7.5 L/min was set to simulate slow inhalation through a single nostril. Experiments were performed in triplicate. After each experiment, the Alberta Idealized Nasal Inlet was disassembled, and each region was washed with appropriate volumes of methanol to break the liposomes and ensure the proper detection of FITC-dextran (λ excitation: 495 nm; λ emission: 525 nm) by spectrophotometer (Lambda 25, PerkinElmer, Milan, Italy).

To qualitatively assess the deposition, anionic liposomes and cationic DOTAP-liposomes were mixed with 20 μL of a solution (2 mg mL^{-1}) of blue patent dye and red ponceau dye, respectively. Pictures were taken after actuating the device in the same conditions reported above.

2.5. In vitro studies with liposomes

2.5.1. Bone marrow-derived dendritic cells and B3Z OT-I hybridoma cell line

Bone marrow dendritic cells were derived by *in vitro* differentiation of myeloid precursors.

Myeloid precursors were isolated by bone marrow of tibiae of eight-week-old female C57BL/6 mice (Charles River Lecco, Italy), housed under standard pathogen-free conditions abiding by institutional guidelines. All animal manipulation and experimental procedures comply with the Arrive guidelines and were carried out in accordance with the European Community guidelines (directive 2010/63) and under the approval of the Italian Ministry of Health (authorization n° 7E58D.12 released on 5-20-2020). Both ends of the tibiae were cut, and bone marrow was flushed with the needle of a syringe filled with ice-cold Roswell Park Memorial Institute (RPMI 1640) medium. Clusters of cells were dissolved by pipetting, and cells were washed twice with medium, plated, and cultured with 200 U mL^{-1} of recombinant murine granulocyte/macrophage colony-stimulating factor (GM-CSF) in RPMI 1640 medium supplemented with 10 % fetal calf serum, 60 μg mL^{-1} penicillin, 100 μg mL^{-1} streptomycin, 1 mM sodium pyruvate, and 50 μM 2-mercaptoethanol. Immature dendritic cells were collected 8 days later and used in the antigen presentation assay.

B3Z OT-I hybridoma cell line was grown in RPMI1640 supplemented with 10 % fetal calf serum, 100 U mL^{-1} penicillin, 100 μg mL^{-1} streptomycin, 1 % glutamine, 1 % non-essential amino-acids, 1 % sodium pyruvate and 50 μM 2-mercaptoethanol. B3Z cells have a T-cell receptor

specific for the ovalbumin-derived peptide 257–264 (SIINFEKL) presented by the major histocompatibility complex I (MHC I) on the surface of dendritic cells [45]. Recognition of the presented peptide by B3Z cells results in the production of interleukin-2 (IL-2), which correlates with the uptake and processing of the ovalbumin and, thus, the antigen presentation [46].

2.5.2. Antigen presentation assay

Dendritic cells (1×10^6 mL^{-1}) were incubated in culture medium (control) or with different concentrations (1–5 μg mL^{-1}) of either ovalbumin-encapsulated liposomes or ovalbumin solution. After overnight incubation, the dendritic cells were co-cultured for 40 h with the B3Z hybridoma cells (5×10^5/well) and the amount of IL-2 released in the medium of co-cultured cells was measured by ELISA. Supernatants (0.1 mL/well) were assayed in duplicate using mouse IL-2 ELISA MAX Standard Set (BioLegend, San Diego, CA). Results are representative of two independent experiments.

2.5.3. Isolation of human monocytes and monocyte-derived macrophages

All samples of human blood included in this study were obtained from anonymous volunteers after informed consent, and all were donated by the hospital "Azienda Ospedaliera Universitaria Federico II" as discarded blood products. Peripheral blood mononuclear cells were separated by Ficoll-Paque gradient density separation (GE Healthcare, Bio-Sciences AB, Uppsala, Sweden) and then monocytes were isolated by CD14 positive selection with magnetic microbeads (Miltenyi Biotec, Bergisch Gladbach, Germany). Monocytes used in the experiments were >95 % viable and >95 % pure (assessed by trypan blue exclusion and cytosmears). 5×10^5 monocytes were seeded in 24-well flat-bottom plates in a final volume of 1 mL/well of RPMI 1640 and Glutamax-I supplemented with 50 μg mL^{-1} gentamicin sulphate, 5 % heat-inactivated AB human serum (Sigma-Aldrich, MO, USA), and 10 ng mL^{-1} macrophage colony-stimulating factor (M-CSF). To obtain differentiated macrophages, the cells were maintained at 37 °C in 5 % CO_2 atmosphere for 7 days. The medium was changed every 3 days.

2.5.4. Biocorona formation on liposome surface

Liposomes were pre-incubated, admixed 1:1 (v/v) with heat-inactivated AB human serum, and incubated for 1 h at 37 °C in an orbital shaker (Thermo-Shaker TS-100C, BioSan, Riga, Latvia) at 300×*g*, in order to obtain the formation of serum protein biocorona on their surface thereby ensuring their stability in culture. The vesicles with the serum shell were added directly to culture wells, and their concentration was adjusted to the desired values for each treatment.

2.5.5. Stimulation of monocyte-derived macrophages

Monocyte-derived macrophages were exposed for 24 h to culture medium alone (negative control), medium containing 5 ng mL^{-1} of lipopolysaccharide from *E. coli* O55:B5 (positive control), medium containing ovalbumin or medium containing biocorona-coated liposomes diluted up to 200 ng mL^{-1}, 1 μg mL^{-1}, 5 μg mL^{-1} of ovalbumin. After exposure, cell supernatants were collected, centrifuged, and frozen at −80 °C for subsequent cytokine analysis. Production of tumor necrosis factor α (TNF-α) was measured in the culture supernatants using an ELISA kit (R&D Systems, MN, USA) according to the manufacturer's protocol and analyzed with a MultiScan FC reader (Thermo Scientific).

2.6. Statistical analysis

Results are expressed as the mean ± standard deviation. Variance analysis was used to determine statistically significant differences among the samples (n = 3 per type). The Tukey-Kramer *t*-test was employed as a post-hoc statistical test to confirm the presence of a significant difference between the means of two specific groups. The statistical analysis was performed by using the Excel software package (Microsoft Corp, Redmond, USA) equipped with a tool for statistical analysis, and the minimum level of significance chosen was $p < 0.05$.

3. Results

3.1. Characterization of liposomes

The actual formation of liposomes, along with their morphology and lamellarity, was confirmed by cryogenic transmission electron microscopy (Fig. 1). Anionic liposomes were overall smaller than cationic DOTAP-liposomes, slightly irregularly shaped, and mostly unilamellar. By contrast, cationic DOTAP-liposomes had an overall more regular and spherical shape and an uni- or oligolamellar structure.

The MD, PDI, ZP, and EE of the vesicles were assessed (Table 1). The anionic liposomes were smaller and more homogeneously dispersed than the cationic DOTAP-liposomes, thus corroborating the observations made through cryogenic transmission electron microscopy. The addition of DOTAP strongly affected the shape and surface charge of the vesicles, which became regular and spherical. The cationic DOTAP-liposomes exhibited a ZP of around 50 mV, in contrast to the ZP of −8 mV observed in the anionic liposomes prepared without it. Despite the anionic liposomes and cationic DOTAP-liposomes being able to encapsulate high amounts of antigen (>70 %), the cationic ones led to higher encapsulation (~82 %), thus suggesting an important role of the DOTAP not only in the superficial charge but also in the vesicle assembling and antigen loading.

The long-term stability of the vesicle dispersions was evaluated by measuring all the physico-chemical variations involving MD, PDI, and ZP during 3 months (Table 2). While the MD and the PDI of the anionic liposomes were basically unaffected over time, a progressive increase in these parameters was observed for the cationic DOTAP-liposomes. This increase could be related to a rearrangement of vesicles, as confirmed by the slight decrease in the ZP. After the 4th month, it was impossible to measure these parameters further because of the precipitation phenomena that occurred in the two dispersions.

The muco-adhesiveness of liposomes was evaluated by diluting the dispersions with a mucin solution (0.5 mg mL^{-1}) and measuring the resulting ZP and the amount of mucin adsorbed on their surface. The initial ZP of anionic liposomes (−8 mV) did not undergo significant changes, becoming only slightly more negative and reaching almost the same values as the mucin dispersion (−18 mV), regardless of the incubation time. On the contrary, the ZP of cationic DOTAP-liposomes underwent a substantial change, shifting from a strong positive value (53 mV) to a significant negative value (−18 mV), similar to that of mucin, regardless of the incubation time. Considering these changes in ZP, it can be concluded that greater interactions occurred between the mucus and cationic DOTAP-liposomes due to their positive charge. The intensity of such interactions was evaluated measuring the amount of mucin adsorbed on vesicle surface after incubation with the same mucin solution (0.5 mg mL^{-1}) for 20 min at 37 °C (Fig. 2). The cationic DOTAP-liposomes adsorbed an 11-fold higher amount of mucin than the anionic liposomes, reaching a mucin adsorption, ~88 %, compared to ~8 % of anionic liposomes.

3.2. Sprayability of liposome dispersions

The adequacy of these formulations to be sprayed and, therefore, used as nasal spray vaccines was first evaluated in terms of variations of MD, PDI, ZP, and EE after nebulization with respect to the initial values (Table 3). Statistical differences could only be found when comparing anionic and DOTAP-liposomes due to the differences in their initial characteristics. By contrast, after nebulization with the Nasonex® device, both vesicles demonstrated high stability as none of the studied parameters (i.e., MD, PDI, and EE) underwent significant variations. Considering that the internal diameter of the nozzle is in the range of 400–800 μm while the MD of both vesicles is < 130 nm, it is likely that no physical obstruction is generated during the actuation of the device.

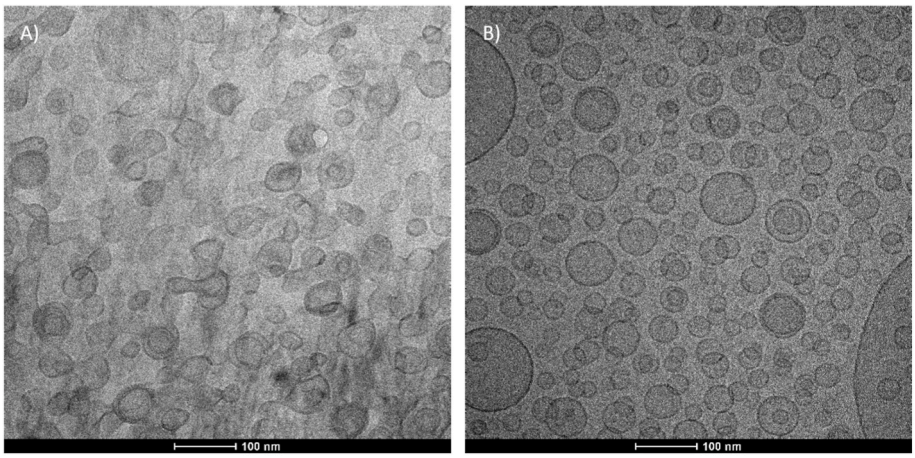

	P90G (mg·mL⁻¹)	DOTAP (mg·mL⁻¹)	Cholesterol (mg·mL⁻¹)	Ovalbumin (mg·mL⁻¹)
Liposomes	69	-	1	5
DOTAP-liposomes	60	9	1	5

Fig. 1. Representative Cryo-TEM images of anionic liposomes (A) and cationic DOTAP-liposomes (B). The liposomal composition (mg·mL^{-1}) is provided (table) to facilitate comparison between the systems.

Table 1
MD, PDI, ZP, and EE of ovalbumin-encapsulated liposomes (mean values ± standard deviations, n = 3).

	MD (nm)	PDI	ZP (mV)	EE (%)
Liposomes	108 ± 1	0.22 ± 0.01	−8±1	74 ± 4
DOTAP-liposomes	125 ± 2	0.26 ± 0.01	53 ± 2	82 ± 1

In addition, for fluids with a viscosity approximately equal to that of water, like these vesicle dispersions, low Reynolds numbers (Re) are generated by the device, which basically correspond to laminar flows (Re < 3100) and not to turbulent flows (Re > 3100) [47]. Consequently, these two elements cannot alter the structural integrity of the vesicles, which is ultimately linked to the retention of the initial physicochemical properties and high encapsulation efficiencies of the antigen (>70 %).

Upon confirmation of vesicle stability under nebulization conditions, the aerosol droplet size generated by the device was characterized following the specifications outlined by the European Medicines Agency (EMA) and the U.S. Food and Drug Administration (FDA) for nasal spray-based vaccine delivery systems. The nozzle tip of the device was positioned at 4 and 7 cm from the laser beam in two consecutive measurements while keeping the device oriented at 45°. The cumulative volumes of undersized droplets, expressed as D10, D50, and D90, were calculated

Table 2
MD, PDI, and ZP of ovalbumin-encapsulated liposomes at 30 and 90 days (mean values ± standard deviations, n = 3).

	MD (nm)			PDI			ZP (mV)		
Days	0	30	90	0	30	90	0	30	90
Liposomes	108 ± 1	106 ± 1	108 ± 3	0.22 ± 0.01	0.23 ± 0.01	0.21 ± 0.02	−8±1	−13 ± 1	−12 ± 2
DOTAP-liposomes	127 ± 2	138 ± 2	140 ± 8	0.25 ± 0.01	0.26 ± 0.01	0.27 ± 0.01	53 ± 2	50 ± 2	46 ± 6

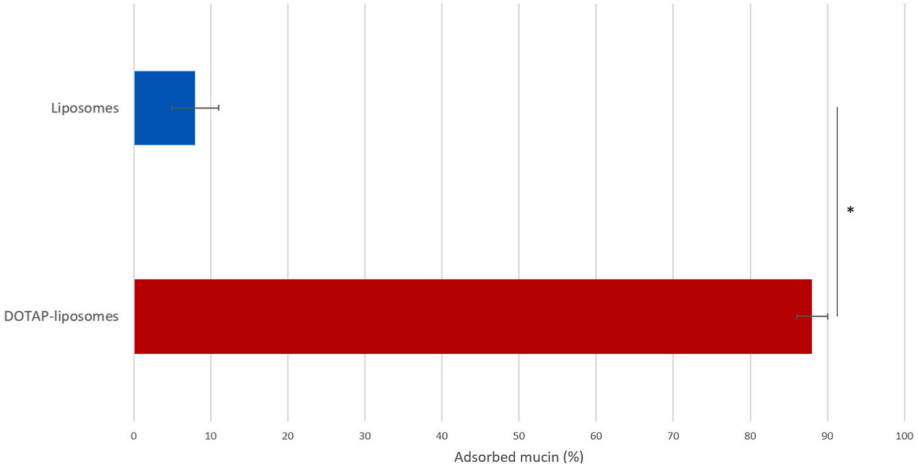

Fig. 2. Percentage of mucin adsorbed on the surface of anionic liposomes (in blue) and cationic DOTAP-liposomes (in red) after their incubation with a mucin solution (0.5 mg mL^{-1}) for 20 min at 37 °C (mean values ± standard deviations, n = 3). The symbol (*) indicates statistically different values ($p < 0.05$). (For interpretation of the references to colour in this figure legend, the reader is referred to the Web version of this article.)

Table 3
MD, PDI, ZP, and EE of ovalbumin-encapsulated liposomes before and after nebulization with the Nasonex® device (mean values ± standard deviations, n = 3). Statistical analysis was performed comparing the data within the same row (before or after nebulization analysis, liposomes vs DOTAP-liposomes) or the same column (before and after nebulization analysis, liposomes vs liposomes and DOTAP-liposomes vs DOTAP-liposomes). Statistically different values ($p < 0.05$) are indicated by symbols (*, □).

		Liposomes	DOTAP-liposomes
Before nebulization	MD (nm)	108 ± 1*	125 ± 2*
	PDI	0.22 ± 0.01*	0.26 ± 0.01*
	ZP (mV)	−8 ± 1*	53 ± 2*
	EE (%)	74 ± 4*	82 ± 1*
After nebulization	MD (nm)	113 ± 3□	123 ± 1□
	PDI	0.24 ± 0.02	0.26 ± 0.01
	ZP (mV)	−11 ± 2□	57 ± 6□
	EE (%)	71 ± 4□	81 ± 5□

along with the width of their size distribution, expressed as span (Fig. 3). Overall, the narrow span values (<1.5) highlighted a high homogeneity of size distribution among the generated droplets. When sprayed at 4 cm from the laser beam, the behaviour of the anionic and cationic DOTAP-liposome dispersions was similar. The D90 was ~90 μm and the D10 was ~22 μm, indicating that 90 % of the generated droplets had a physical diameter ≤90 μm and the remaining 10 % had a diameter ≤22 μm. When the dispersions were sprayed at 7 cm from the laser beam, the D90 decreased to ~78 μm while the D10 increased to ~30 μm. The D50 was the only value unaffected by the laser beam distance or the dispersion used, remaining constant at ~50 μm. However, regardless of the tested distance or formulation, the generated droplets were always larger than 10 μm and, therefore, suitable to be deposited in the nasal cavity [48].

3.3. *In vitro deposition of liposome dispersions using the Alberta Idealized Nasal Inlet*

The specific regional deposition of anionic liposomes and cationic DOTAP-liposomes was then assessed using a realistic nasal replica, the AINI, which possesses a four-region resolution (vestibule, olfactory region, turbinates, and nasopharynx) to allow the recovery of the sample, connected to the NGI, which simulates the lungs (Fig. 4) [36]. The quantitative recovery was confirmed qualitatively using blue patent dye-labelled anionic liposomes and red ponceau dye-labelled cationic DOTAP-liposomes. To facilitate the quantification, liposomes were

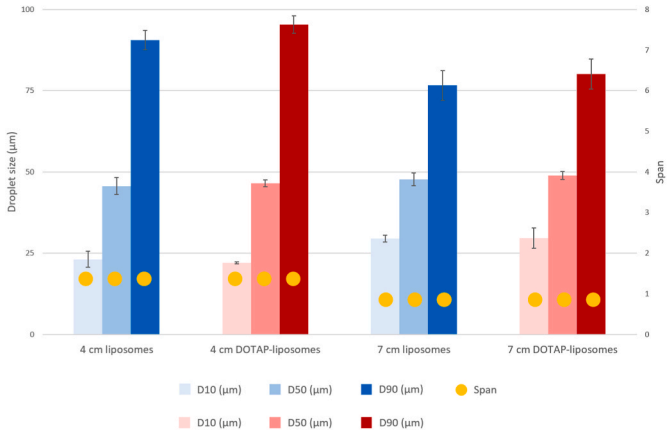

Fig. 3. Cumulative volumes of undersized droplets (D10, D50, and D90) and width of their size distribution (span) for anionic liposomes (blue) and DOTAP-liposomes (red) sprayed at distances of 4 cm (left bars) and 7 cm (right bars) from the laser beam (mean values ± standard deviations, n = 3). (For interpretation of the references to colour in this figure legend, the reader is referred to the Web version of this article.)

fluorescently labelled with FITC-dextran. The total recovery of the labelled vesicles was ~95 %, irrespective of the formulation. The deposition of anionic liposomes and cationic DOTAP-liposomes in the vestibule was ~45 %, with no statistical differences between the values obtained with the two formulations ($p > 0.05$). Similarly, using the two different formulations, the deposition in the olfactory region (<0.5 %) and in the lungs (0 %) was not statistically different. By contrast, in the turbinates, the deposition provided by cationic DOTAP-liposomes (~52 %) was significantly higher than that provided by anionic liposomes (~43 %, $p < 0.05$ between the two values). In the nasopharynx, the deposition of anionic liposomes was slightly higher (~3 %) than that of cationic DOTAP-liposomes (~0.8 %, $p < 0.05$ between the two values). Considering these findings, the similar deposition patterns observed for both anionic and cationic DOTAP-liposomes in the vestibule suggest that the effect of surface charge may be attenuated or even masked within this region. The high velocity imparted by the spray device in this first stage of the AINI likely results in a deposition mechanism dominated by inertial impaction, rather than electrostatic interactions. Conversely, in more distal regions such as the turbinates, the diminished velocity enables droplets to align with the airflow, potentially increasing the chance for vesicles to interact with the mucin layer. Consequently, the greater deposition of cationic DOTAP-liposomes that occurs in the turbinates is possibly facilitated by more pronounced electrostatic forces with the negatively charged mucin, in comparison to anionic liposomes, which possess the same charge as mucin and are repulsed towards the last stage of the AINI (i.e., the nasopharynx).

3.4. *In vitro tests*

3.4.1. *IL-2 production by OVA$_{(257-264)}$-specific B3Z cells*

The efficacy of anionic liposomes and cationic DOTAP-liposomes as antigen delivery carriers was evaluated measuring the IL-2 produced in a co-culture of dendritic cells exposed to liposome dispersions or culture medium (control) and B3Z cells (Fig. 5). When the ovalbumin solution was used, the production of IL-2 was negligible and comparable to that found in the control cells exposed to the medium without the antigen (≈15 pg mL^{-1}, $p > 0.05$ between the two values), irrespective of the used concentration. An increased production of IL-2 was detected when the ovalbumin was delivered in anionic liposomes, regardless of the used concentration (≈85 pg mL^{-1}, $p > 0.05$ between the two values). A further increase was found in delivering ovalbumin in cationic DOTAP-liposomes, as the concentration was ~120 pg mL^{-1} with 1 μg mL^{-1} and ~137 pg mL^{-1} with 5 μg mL^{-1} (≈85 pg mL^{-1}, $p > 0.05$ versus 137 pg mL^{-1}). Results indicate that both formulations, especially cationic DOTAP-liposomes, mediated antigen uptake, processing, and presentation as they induced IL-2 production at levels significantly higher than those provided by the ovalbumin solution.

3.4.2. *Production of TNF-α by human monocyte-derived macrophages*

The inflammatory response was evaluated after exposing human monocyte-derived macrophages for 24 h to ovalbumin in solution or encapsulated in anionic liposomes or cationic DOTAP-liposomes. Three dilutions were tested corresponding to 200 ng mL^{-1} (data not shown), 1 μg mL^{-1} (data not shown), and 5 μg mL^{-1} (Fig. 6) of ovalbumin. Macrophages exposed only to the culture medium were used as a negative control, whereas macrophages exposed to lipopolysaccharide, a prototypical inflammatory stimulus, were used as a positive control. Macrophage activation was evaluated by measuring the production of the inflammatory cytokine TNF-α. Similarly to the ovalbumin solution, the ovalbumin-encapsulated liposomes did not induce a measurable reactivity in human macrophages, being unable to promote TNF-α and thus an inflammatory response at any tested dose ($p < 0.05$).

4. Discussion

With the aim of formulating liposomes tailored to be easily

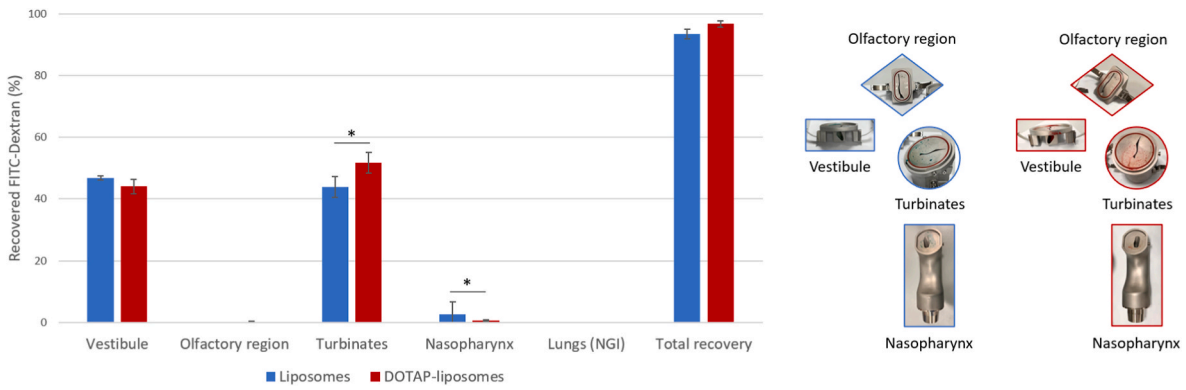

Fig. 4. FITC-dextran recovered in the deposition regions of the AINI (vestibule, olfactory region, turbinates, and nasopharynx) and the NGI (lungs) after nebulization of labelled anionic liposomes (in blue) and cationic DOTAP-liposomes (in red) (mean values ± standard deviations, n = 3). The symbol (*) indicates statistically different values ($p < 0.05$). (For interpretation of the references to colour in this figure legend, the reader is referred to the Web version of this article.)

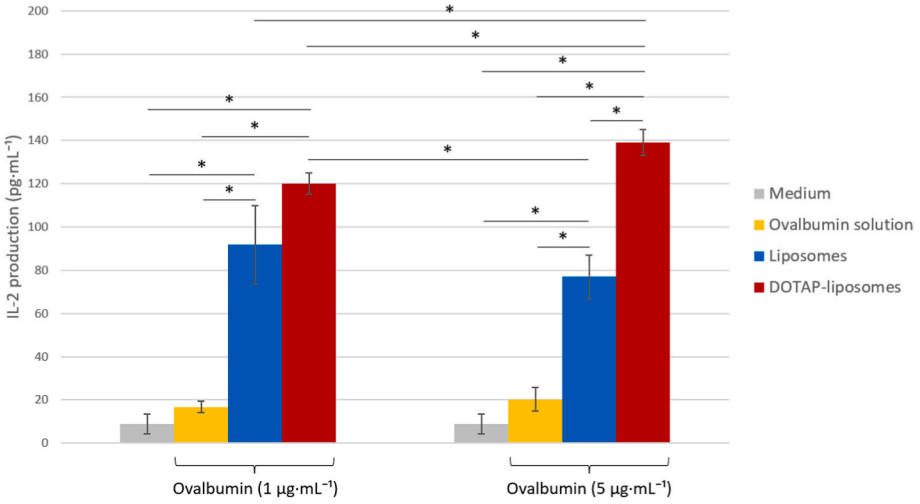

Fig. 5. IL-2 measured in the medium of dendritic cells pre-exposed to culture medium (control), ovalbumin solution (1 and 5 µg mL^{-1}) or ovalbumin (1 and 5 µg mL^{-1}) encapsulated in anionic liposomes or cationic DOTAP-liposomes and co-cultured with B3Z cells (mean values ± standard deviations representative of two independent experiments). The symbol (*) indicates statistically different values ($p < 0.05$).

administered intranasally to stimulate immunity at the nasal level and block the pathogens at the entry site, the model antigen ovalbumin was encapsulated in two kinds of phospholipid vesicles, having negative (liposomes) and positive (DOTAP-liposomes) superficial charge. Primary importance was devoted to the selection of vesicle composition, which strongly affects vesicle performances and surface charge, ultimately playing a key role in mucus adhesion, particle retainment in situ, and cellular uptake by the antigen-presenting cells of the immune system. Thus, a commercial mixture of phosphatidylcholines (P90G) was selected and used as a main lipidic component by virtue of their uptake-enhancing properties, whereas DOTAP, a cationic phospholipid featuring an unsaturated fatty acid, was chosen to impart positive charge and induce the immune response [49,50]. Currently, cationic liposomes have gained attention as adjuvants for vaccine delivery as they can boost antigen delivery and promote antigenic protein uptake by antigen-presenting cells [30,51]. Although the mechanism of their adjuvanticity is not fully understood, what is well known is the ability of DOTAP to promote cell surface contact by electrostatic interaction, foster uptake and antigen presentation by dendritic cells and even increase the humoral response [26]. During the preparation of the ovalbumin-encapsulated liposomes, cholesterol was also added to P90G and DOTAP because of its membrane-stabilizing effects [52]. By contrast, positively charged cholesterol, which has also been used to produce vaccines, was not considered for this study because of its higher cost and its toxicity in combination with DOTAP, as reported by several authors [35,53–55].

Irrespective of the formulation, direct sonication was used as an organic solvent-free and eco-friendly method to prepare the phospholipid vesicles [56,57]. The chosen method was consistent, allowing to obtain homogeneous systems (PDI <0.3) with high EE (>70 %) as much as other techniques such as thin film evaporation, ethanol injection, and microfluidics, which, however, rely on organic solvents to dissolve lipids and are therefore not environmentally safe and require several dissipative preparation steps [19].

As most vaccines nowadays struggle to ensure a palatable route of administration that is painless and non-invasive, the nasal route was elected to administer ovalbumin-encapsulated liposomes to the nasal cavity and elicit a response in situ. This is currently regarded as a promising preventive strategy, especially against those diseases affecting the respiratory system, which is often exposed to airborne pathogens [58]. However, liposomes must stay stable upon nebulization and not lose their payload to be truly effective. The findings of the current study highlighted the high degree of structural retainment of the obtained vesicles upon nebulization with the commercial spray device Nasonex® and, therefore, their suitability to be sprayed with this device. The absence of high shear forces generated by the device and the high flexibility of these vesicular systems are reported as key factors in ensuring suitable delivery of the payloads through the nose [20,47].

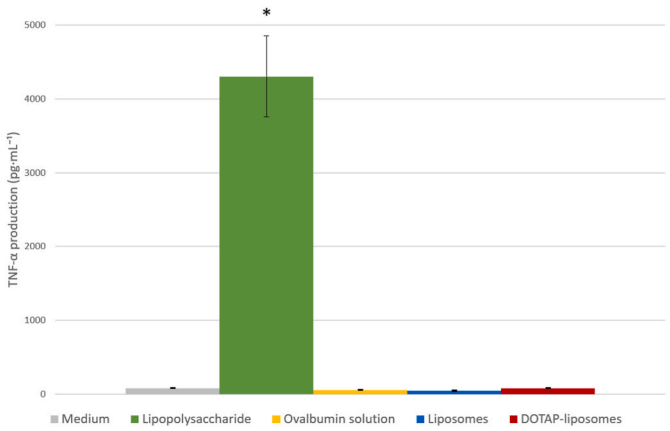

Fig. 6. TNF-α produced by human monocyte-derived macrophages exposed to the culture medium (in grey, negative control), ovalbumin solution (5 μg mL^{-1}) (in yellow) or ovalbumin (5 μg mL^{-1}) encapsulated in anionic liposomes (in blue), and DOTAP-liposomes (in red) or 5 ng mL^{-1} of lipopolysaccharide (in green, positive control) (mean values ± standard deviations representative of two independent experiments). The symbol (*) indicates statistically different values from all the other treatments ($p < 0.05$). (For interpretation of the references to colour in this figure legend, the reader is referred to the Web version of this article.)

Nonetheless, in evaluating nasal performance, it is also important to have a general understanding of the deposition phenomena, which is why the EMA and FDA suggest assessing the droplet size distribution [59,60]. The results obtained in this study indicated that both formulations, once sprayed, generated droplets larger than 10 μm, with up to the 90 % of the droplets lying in a dimensional range of 80–90 μm. Being 5 μm the required aerodynamic diameter to ensure lung deposition, the data collected highlighted that a high percentage of droplets was deposited nasally with extreme precision, avoiding any pulmonary deposition [48]. The characterization of the specific deposition site in the nose was further carried out with the AINI, whose geometry allows the assessment of deposited materials in four anatomical regions (vestibule, turbinates, olfactory region, and nasopharynx) with high correlation *in vitro-in vivo* [61]. According to the results of a previous study performed by Chen and colleagues, the obtained data indicated that the droplets generated by the device deposited in the nose but not in the lungs [61]. Specifically, the percentage of anionic liposomes and cationic DOTAP-liposomes detected in the vestibule was comparable (~45 %), whereas that of cationic DOTAP-liposomes in the turbinates was higher (~52 %). In a vaccine context, the deposition in the posterior nasal cavity (i.e., turbinates) is recognized as the site where the immune response is mainly produced [62,63]. Accordingly, Xu and colleagues achieved better *in vivo* efficacy of their vaccine candidate when it was more effectively deposited in the turbinate region during *in vitro* studies on a nasal replica [64]. Consequently, the cationic DOTAP-liposomes are expected to be more suitable than the anionic ones since their higher muco-adhesiveness (88 % vs ~8 %) led to a higher deposition in this region of the posterior nasal cavity [32,65].

Even though deposition in this area can improve vaccine effectiveness, it alone is insufficient to ensure a proper immune response. The improved capability of the carriers to deliver the antigen to the antigen-presenting cells is mandatory, as these cells process the antigen and present it to the lymphocytes, thereby initiating the immune response [66]. IL-2 modulates regulatory T cells and tunes effector lymphocyte responses, two important processes involved in immunological responses. Therefore, bone marrow-derived dendritic cells were exposed to two different concentrations of ovalbumin (5 and 1 μg mL^{-1}) in solution or encapsulated in phospholipid vesicles, and the antigen uptake, processing, and presentation were evaluated by measuring IL-2 production by the co-cultured T cells. Ovalbumin loaded in liposomes significantly boosted IL-2 production compared to the antigen solution, confirming the carrier's ability to be effectively sensed and engulfed by the antigen-presenting cells. In particular, cationic DOTAP-liposomes provided the highest production of IL-2 in a concentration-dependent manner. The differences in the response efficiency were probably mediated by the surface charge of vesicles. Indeed, as reported elsewhere, positively charged liposomes display greater adjuvanticity than negatively charged or neutral liposomes due to their better ability to interact with the negatively charged membranes of antigen-presenting cells [67,68].

The introduction of foreign materials, such as vaccines, into the organism, may be sensed by the innate immune system as a harmful stimulus. In this respect, the formulations used did not trigger an inflammatory response in human macrophages, as no production of the inflammatory cytokine TNF-α was detected [69]. Although measuring a single inflammatory cytokine is not exhaustive, the lack of response at any dilution of ovalbumin, whether in solution or encapsulated in liposomes, suggests that the carriers themselves do not exert proinflammatory effects following administration and are perceived as safe by the immune system [70–72]. According to Bygd and colleagues, the composition of liposomes can alter macrophage phenotype and their responses [73]. Tada et al. used a combination of DOTAP and cholesterol in cationic liposomes and did not observe an altered response, as no TNF-α expression was detected upon administration [30]. On the other hand, Li and co-workers developed anionic liposomes using phosphatidylcholine as the main lipid, observing that TNF-α production was, again, not influenced upon exposure [74]. In this study, liposomes were mainly composed of phosphatidylcholine and cholesterol, alone (anionic liposomes) or in combination with DOTAP (cationic DOTAP-liposomes), and no TNF-α response was detected. Therefore, the anionic liposomes and cationic DOTAP-liposomes developed here have a suitable composition, as they are unable to trigger a potential inflammatory response upon administration, confirming previous findings.

5. Conclusions

The results of this study demonstrate that ovalbumin can be successfully encapsulated in anionic liposomes and cationic DOTAP-liposomes via water dispersion and direct sonication. This method avoids dissipative preparation steps and organic solvents, offering a simple, eco-friendly manufacturing process using primarily natural components such as soy phosphatidylcholine and cholesterol. The formulations, sprayed with a commercial nasal device, are widely stable upon nebulization, allowing the encapsulated antigen to be retained after the device actuation. Cationic DOTAP-liposomes are particularly promising, achieving primary deposition in the turbinates and enhancing antigen delivery and presentation while being well-tolerated. Overall, they also appear more suitable for nasal administration due to their higher muco-adhesiveness, potentially leading to a prolonged local response. However, *in vivo* studies are needed to confirm the promise of this ovalbumin formulation. Possibly, a dried form will be developed in the future to extend its storage and use.

CRediT authorship contribution statement

Matteo Aroffu: Writing – original draft, Visualization, Methodology, Investigation, Formal analysis, Data curation. **Federica Fulgheri:** Writing – review & editing, Validation, Methodology, Investigation. **Rita Abi Rached:** Writing – review & editing, Validation, Methodology. **Ines Castangia:** Writing – review & editing, Methodology. **Annunziata Corteggio:** Validation, Methodology, Investigation. **Paola Italiani:** Writing – review & editing, Validation, Methodology, Investigation. **Luciana D'Apice:** Writing – review & editing, Validation, Methodology, Investigation. **Myriam Sainz-Ramos:** Validation, Methodology, Investigation. **Fátima García-Villén:** Validation, Methodology, Investigation. **Xavier Fernàndez-Busquets:** Validation, Methodology,

Investigation. **Maria Manconi:** Writing – review & editing, Visualization, Validation, Supervision, Project administration, Methodology, Conceptualization. **José Luis Pedraz:** Writing – review & editing, Visualization, Validation, Supervision, Project administration, Methodology, Conceptualization. **Maria Letizia Manca:** Writing – review & editing, Visualization, Validation, Supervision, Project administration, Methodology. **Anna Maria Fadda:** Writing – review & editing, Visualization, Validation, Supervision, Methodology, Funding acquisition.

Declaration of competing interest

The authors declare that they have no known competing financial interests or personal relationships that could have appeared to influence the work reported in this paper.

Acknowledgments

This research was comprehensively supported by the Project PRIN 2017, n. 20173ZECCM, "*Tackling biological barriers to antigen delivery by nanotechnological vaccines (NanoTechVax)*", funded by the Italian Ministry of University and Research. The authors are also grateful for the support and the expertise provided by the ICTS "NANBIOSIS" and the Drug Formulation Unit (U10) of the CIBER in Bioengineering, Biomaterials and Nanomedicine (CIBER-BBN), and consolidated groups (IT1448-22) at the University of Basque Country (UPV/EHU).

Abbreviations

Abbreviation	Full-length text
AINI	Alberta Idealized Nasal Inlet
BCA protein assay kit	Bicinchoninic acid protein assay kit
DOTAP	Dioleoyl-3-trimethylammonium propane
EE	Encapsulation efficiency
FITC-dextran	Fluorescein isothiocyanate-dextran
GM-CSF	Murine granulocyte/macrophage colony-stimulating factor
IL-2	Interleukin-2
MD	Mean diameter
NGI	Next Generation Impactor
P90G	Phospholipon® 90G
PDI	Polidispersity index
Re	Reynolds numbers
RPMI 1640	Roswell Park Memorial Institute 1640
TNF-α	Tumor necrosis factor-α
ZP	Zeta potential

Data availability

The authors have chosen not to specify which data has been used.

References

[1] M. Lombard, P.P. Pastoret, A.M. Moulin, A brief history of vaccines and vaccination, OIE Revue Scientifique et Technique 26 (2007) 29–48, https://doi.org/10.20506/rst.26.1.1724.
[2] J.H. Silverstein, F.T. Murray, T. Malasanos, S. Myers, S.B. Johnson, K. Frye, M. Grossman, Clinical testing results and high patient satisfaction with a new needle-free device for growth hormone in young children, Endocrine 15 (2001) 15–17, https://doi.org/10.1385/endo:15:1s:s15.
[3] A.M. Mayo, S. Cobler, Flu vaccines and patient decision making: what we need to know, J. Am. Acad. Nurse Pract. 16 (2004) 402–410, https://doi.org/10.1111/j.1745-7599.2004.tb00390.x.
[4] H. Le, R.B. Vender, A Psoriatic Patient-based survey on the understanding of the use of vaccines while on biologics during the COVID-19 pandemic, J. Cutan. Med. Surg. 25 (2021) 298–302, https://doi.org/10.1177/1203475421991126.
[5] U.U. Shah, M. Roberts, M. Orlu Gul, C. Tuleu, M.W. Beresford, Needle-free and microneedle drug delivery in children: a case for disease-modifying antirheumatic drugs (DMARDs), Int. J. Pharm. 416 (2011) 1–11, https://doi.org/10.1016/j.ijpharm.2011.07.002.
[6] E.H. Moeller, L. Jorgensen, Alternative routes of administration for systemic delivery of protein pharmaceuticals, Drug Discov. Today Technol. 5 (2008) e89–e94, https://doi.org/10.1016/j.ddtec.2008.11.005.
[7] E.M. Coma-Cros, A. Biosca, E. Lantero, M.L. Manca, C. Caddeo, L. Gutiérrez, M. Ramírez, L.N. Borgheti-Cardoso, M. Manconi, X. Fernàndez-Busquets, Antimalarial activity of orally administered curcumin incorporated in eudragit®-containing liposomes, Int. J. Mol. Sci. 19 (2018) 1361, https://doi.org/10.3390/ijms19051361.
[8] M.L. Manca, M. Zaru, M. Manconi, F. Lai, D. Valenti, C. Sinico, A.M. Fadda, Glycerosomes: a new tool for effective dermal and transdermal drug delivery, Int. J. Pharm. 455 (2013) 66–74, https://doi.org/10.1016/j.ijpharm.2013.07.060.
[9] E. Casula, M.L. Manca, M. Perra, J.L. Pedraz, T.B. Lopez-Mendez, A. Lozano, E. Calvo, M. Zaru, M. Manconi, Nasal spray formulations based on combined hyalurosomes and glycerosomes loading zingiber officinalis extract as green and natural strategy for the treatment of rhinitis and rhinosinusitis, Antioxidants 10 (2021) 1109, https://doi.org/10.3390/antiox10071109.
[10] Y.Y. Huang, C.H. Wang, Pulmonary delivery of insulin by liposomal carriers, J. Contr. Release 113 (2006) 9–14, https://doi.org/10.1016/j.jconrel.2006.03.014.
[11] A. Kumar, A.N. Pandey, S.K. Jain, Nasal-nanotechnology: revolution for efficient therapeutics delivery, Drug Deliv. 23 (2016) 671–683, https://doi.org/10.3109/10717544.2014.920431.
[12] M. Tafaghodi, M.R. Jaafari, S.A. Sajadi Tabassi, Nasal immunization studies using liposomes loaded with tetanus toxoid and CpG-ODN, Eur. J. Pharm. Biopharm. 64 (2006) 138–145, https://doi.org/10.1016/j.ejpb.2006.05.005.
[13] M. Ishii, N. Kojima, Mucosal adjuvant activity of oligomannose-coated liposomes for nasal immunization, Glycoconj. J. 27 (2010) 115–123, https://doi.org/10.1007/s10719-009-9263-8.
[14] R. Bajracharya, J.G. Song, S.Y. Back, H.K. Han, Recent advancements in non-invasive formulations for protein drug delivery, Comput. Struct. Biotechnol. J. 17 (2019) 1290–1308, https://doi.org/10.1016/j.csbj.2019.09.004.
[15] J.R. Baker, M. Farazuddin, P.T. Wong, J.J. O'Konek, The unfulfilled potential of mucosal immunization, J. Allergy Clin. Immunol. 150 (2022) 1–11, https://doi.org/10.1016/j.jaci.2022.05.002.
[16] M.A. Sarkar, Drug metabolism in the nasal mucosa, Pharm. Res.: An Official Journal of the American Association of Pharmaceutical Scientists 9 (1992) 1–9, https://doi.org/10.1023/A:1018911206646.
[17] F. Fulgheri, M.L. Manca, X. Fernàndez-Busquets, M. Manconi, Analysis of complementarities between nanomedicine and phytodrugs for the treatment of malarial infection, Nanomedicine (2023) 1681–1696, https://doi.org/10.2217/nnm-2023-0116.
[18] H. Nsairat, D. Khater, U. Sayed, F. Odeh, A. Al Bawab, W. Alshaer, Liposomes: structure, composition, types, and clinical applications, Heliyon 8 (2022) e09394, https://doi.org/10.1016/j.heliyon.2022.e09394.
[19] M. Aroffu, M.L. Manca, J.L. Pedraz, M. Manconi, Liposome-based vaccines for minimally or noninvasive administration: an update on current advancements, Expet Opin. Drug Deliv. 20 (2023) 1573–1593, https://doi.org/10.1080/17425247.2023.2288856.
[20] V.A. Duong, T.T.L. Nguyen, H.J. Maeng, Recent advances in intranasal liposomes for drug, gene, and vaccine delivery, Pharmaceutics 15 (2023) 207, https://doi.org/10.3390/pharmaceutics15010207.
[21] N. Marasini, M. Skwarczynski, I. Toth, Intranasal delivery of nanoparticle-based vaccines, Ther. Deliv. 8 (2017) 151–167, https://doi.org/10.4155/tde-2016-0068.
[22] W.C. Huang, K. Chiem, L. Martinez-Sobrido, J.F. Lovell, Intranasal immunization with liposome-displayed receptor-binding domain induces mucosal immunity and

protection against SARS-CoV-2, Pathogens 11 (2022) 1035, https://doi.org/10.3390/pathogens11091035.
[23] Y. Fan, P. Sahdev, L.J. Ochyl, J.J. Akerberg, J.J. Moon, Cationic liposome-hyaluronic acid hybrid nanoparticles for intranasal vaccination with subunit antigens, J. Contr. Release 208 (2015) 121–129, https://doi.org/10.1016/j.jconrel.2015.04.010.
[24] C.C. Dai, J. Yang, W.M. Hussein, L. Zhao, X. Wang, Z.G. Khalil, R.J. Capon, I. Toth, R.J. Stephenson, Polyethylenimine: an intranasal adjuvant for liposomal Peptide-based subunit Vaccine against group A *Streptococcus*, ACS Infect. Dis. 6 (2020) 2502–2512, https://doi.org/10.1021/acsinfecdis.0c00452.
[25] R. Tada, H. Suzuki, S. Takahashi, Y. Negishi, H. Kiyono, J. Kunisawa, Y. Aramaki, Nasal vaccination with pneumococcal surface protein A in combination with cationic liposomes consisting of DOTAP and DC-chol confers antigen-mediated protective immunity against Streptococcus pneumoniae infections in mice, Int. Immunopharmacol. 61 (2018) 385–393, https://doi.org/10.1016/j.intimp.2018.06.027.
[26] Y. Mai, J. Guo, Y. Zhao, S. Ma, Y. Hou, J. Yang, Intranasal delivery of cationic liposome-protamine complex mRNA vaccine elicits effective anti-tumor immunity, Cell. Immunol. 354 (2020) 104143, https://doi.org/10.1016/j.cellimm.2020.104143.
[27] Z. Kakhi, B. Frisch, B. Heurtault, F. Pons, Liposomal constructs for antitumoral vaccination by the nasal route, Biochimie 130 (2016) 14–22, https://doi.org/10.1016/j.biochi.2016.07.003.
[28] H. Yusuf, A.A. Ali, N. Orr, M.M. Tunney, H.O. McCarthy, V.L. Kett, Novel freeze-dried DDA and TPGS liposomes are suitable for nasal delivery of vaccine, Int. J. Pharm. 533 (2017) 179–186, https://doi.org/10.1016/j.ijpharm.2017.09.011.
[29] H.W. Wang, P.L. Jiang, S.F. Lin, H.J. Lin, K.L. Ou, W.P. Deng, L.W. Lee, Y.Y. Huang, P.H. Liang, D.Z. Liu, Application of galactose-modified liposomes as a potent antigen presenting cell targeted carrier for intranasal immunization, Acta Biomater. 9 (2013) 5681–5688, https://doi.org/10.1016/j.actbio.2012.11.007.
[30] R. Tada, A. Hidaka, N. Iwase, S. Takahashi, Y. Yamakita, T. Iwata, S. Muto, E. Sato, N. Takayama, E. Honjo, H. Kiyono, J. Kunisawa, Y. Aramaki, P.N. Boyaka, Intranasal immunization with dotap cationic liposomes combined with DC-cholesterol induces potent antigen-specific mucosal and systemic immune responses in mice, PLoS One 10 (2015) 1–21, https://doi.org/10.1371/journal.pone.0139785.
[31] R. Tada, S. Muto, T. Iwata, A. Hidaka, H. Kiyono, J. Kunisawa, Y. Aramaki, Attachment of class B CpG ODN onto DOTAP/DC-chol liposome in nasal vaccine formulations augments antigen-specific immune responses in mice, BMC Res. Notes 10 (2017) 68, https://doi.org/10.1186/s13104-017-2380-8.
[32] E.K. Wasan, J. Syeda, S. Strom, J. Cawthray, R.E. Hancock, K.M. Wasan, V. Gerdts, A lipidic delivery system of a triple vaccine adjuvant enhances mucosal immunity following nasal administration in mice, Vaccine 37 (2019) 1503–1515, https://doi.org/10.1016/j.vaccine.2019.01.058.
[33] M. Aroffu, R.A. Rached, I. Castangia, P. Italiani, L. D'Apice, X. Fernàndez-Busquets, A. Nacher, M. Manconi, J.L. Pedraz, M.L. Manca, A preliminary investigation on hydrogel disks imbibed with enriched transfersomes as promising tool to promote the cutaneous deposition of vaccine antigens, J. Drug Deliv. Sci. Technol. 102 (2024) 106399, https://doi.org/10.1016/j.jddst.2024.106399.
[34] E. Yuba, K. Kono, Nasal delivery of biopharmaceuticals, in: J. das Neves, B. Sarmento (Eds.), Mucosal Delivery of Biopharmaceuticals: Biology, Challenges and Strategies, Springer, New York, NY, New York, 2014, pp. 197–220, https://doi.org/10.1007/978-1-4614-9524-6_8.
[35] R. Tada, A. Hidaka, H. Kiyono, J. Kunisawa, Y. Aramaki, Intranasal administration of cationic liposomes enhanced granulocyte-macrophage colony-stimulating factor expression and this expression is dispensable for mucosal adjuvant activity, BMC Res. Notes 11 (2018) 472, https://doi.org/10.1186/s13104-018-3591-3.
[36] Copley, Alberta idealised Nasal Inlet (AINI), (n.d.). https://www.copleyscientific.com/inhaler-testing/realistic-throat-and-nasal-models/alberta-idealised-nasal-inlet-aini/(accessed August 29, 2025).
[37] E. Casula, M. Manconi, T.B. Lopez-Mendez, J.L. Pedraz, E. Calvo, A. Lozano, M. Zaru, I. Castangia, G. Orrù, S. Fais, M.L. Manca, Complementary effect of Zingiber officinalis extract and citral in counteracting non allergic nasal congestion by simultaneous loading in ad hoc formulated phospholipid vesicles, Colloids Surf. B Biointerfaces 209 (2022) 112170, https://doi.org/10.1016/j.colsurfb.2021.112170.
[38] F. Fulgheri, M. Ramírez, L. Román-Álamo, P. Gasco, M. Manconi, M. Aroffu, R. A. Rached, B. Baroli, X. Fernàndez-Busquets, M.L. Manca, Preliminary evaluation of the in vitro and in vivo efficacy of a novel nanovesicle-doped nanoemulsion co-loading artemisinin and quercetin as a promising strategy to improve the oral malaria therapy, J. Drug Deliv. Sci. Technol. 107 (2025) 106828, https://doi.org/10.1016/J.JDDST.2025.106828.
[39] D.W. Greening, R.J. Simpson, Low-Molecular weight plasma proteome analysis using centrifugal ultrafiltration, pp. 109–124, https://doi.org/10.1007/978-1-61779-068-3_6, 2011.
[40] R. Bo, Y. Sun, S. Zhou, N. Ou, P. Gu, Z. Liu, Y. Hu, J. Liu, D. Wang, Simple nanoliposomes encapsulating Lycium barbarum polysaccharides as adjuvants improve humoral and cellular immunity in mice, Int. J. Nanomed. 12 (2017) 6289–6301, https://doi.org/10.2147/IJN.S136820.
[41] E. Hagesaether, M.I. Adamczak, M. Hiorth, I. Tho, Characterization of bioadhesion, mucin-interactions and mucosal permeability of pharmaceutical nano- and microsystems, in: L. Peltonen (Ed.), Characterization of Pharmaceutical Nano and Microsystems, John Wiley & Sons Ltd., 2021, pp. 171–205, https://doi.org/10.1002/9781119414018.ch5.
[42] L. Salade, N. Wauthoz, M. Deleu, M. Vermeersch, C. De Vriese, K. Amighi, J. Goole, Development of coated liposomes loaded with ghrelin for nose-to-brain delivery for the treatment of cachexia, Int. J. Nanomed. 12 (2017) 8531–8543, https://doi.org/10.2147/IJN.S147650.
[43] S. Gänger, K. Schindowski, Tailoring formulations for intranasal nose-to-brain delivery: a review on architecture, physico-chemical characteristics and mucociliary clearance of the nasal olfactory mucosa, Pharmaceutics 10 (2018) 116, https://doi.org/10.3390/pharmaceutics10030116.
[44] L. Shi, K.D. Caldwell, Mucin adsorption to hydrophobic surfaces, J. Colloid Interface Sci. 224 (2000) 372–381, https://doi.org/10.1006/jcis.2000.6724.
[45] A. Desalvo, F. Bateman, E. James, H. Morgan, T. Elliott, Time-resolved microwell cell-pairing array reveals multiple T cell activation profiles, Lab Chip 20 (2020) 3772–3783, https://doi.org/10.1039/d0lc00628a.
[46] M. Pei, R. Xu, C. Zhang, X. Wang, C. Li, Y. Hu, Mannose-functionalized antigen nanoparticles for targeted dendritic cells, accelerated endosomal escape and enhanced MHC-I antigen presentation, Colloids Surf. B Biointerfaces 197 (2021) 111378, https://doi.org/10.1016/j.colsurfb.2020.111378.
[47] G.M. Eccleston, N.E. Hudson, The use of a capillary rheometer to determine the shear and extensional flow behaviour of Nasal Spray suspensions, J. Pharm. Pharmacol. 52 (2000) 1223–1232, https://doi.org/10.1211/0022357001777351.
[48] L. Salade, N. Wauthoz, J. Goole, K. Amighi, How to characterize a nasal product. The state of the art of in vitro and ex vivo specific methods, Int. J. Pharm. 561 (2019) 47–65, https://doi.org/10.1016/j.ijpharm.2019.02.026.
[49] M. Ghadiri, P.M. Young, D. Traini, Strategies to enhance drug absorption via nasal and pulmonary routes, Pharmaceutics 11 (2019) 113, https://doi.org/10.3390/pharmaceutics11030113.
[50] L. Huang, M. Cai, X. Xie, Y. Chen, X. Luo, Uptake enhancement of curcumin encapsulated into phosphatidylcholine- shielding micelles by cancer cells, J. Biomater. Sci. Polym. Ed. 25 (2014) 1407–1424, https://doi.org/10.1080/09205063.2014.941261.
[51] P. Zamani, A.A. Momtazi-Borojeni, M.E. Nik, R.K. Oskuee, A. Sahebkar, Nanoliposomes as the adjuvant delivery systems in cancer immunotherapy, J. Cell. Physiol. 233 (2018) 5189–5199, https://doi.org/10.1002/jcp.26361.
[52] P. Nakhaei, R. Margiana, D.O. Bokov, W.K. Abdelbasset, M.A. Jadidi Kouhbanani, R.S. Varma, F. Marofi, M. Jarahian, N. Beheshtkhoo, Liposomes: structure, biomedical applications, and stability parameters with emphasis on cholesterol, Front. Bioeng. Biotechnol. 9 (2021) 705866, https://doi.org/10.3389/fbioe.2021.705886.
[53] R. Tada, A. Ohshima, Y. Tanazawa, A. Ohmi, S. Takahashi, H. Kiyono, J. Kunisawa, Y. Aramaki, Y. Negishi, Essential role of host double-stranded DNA released from dying cells by cationic liposomes for mucosal adjuvanticity, Vaccines (Basel) 8 (2020) 8, https://doi.org/10.3390/vaccines8010008.
[54] W. Qu, N. Li, R. Yu, W. Zuo, T. Fu, W. Fei, Y. Hou, Y. Liu, J. Yang, Cationic DDA/TDB liposome as a mucosal vaccine adjuvant for uptake by dendritic cells in vitro induces potent humoural immunity, Artif. Cells, Nanomed. Biotechnol. 46 (2018) 852–860, https://doi.org/10.1080/21691401.2018.1438450.
[55] N. Filipczak, J. Pan, S.S.K. Yalamarty, V.P. Torchilin, Recent advancements in liposome technology, Adv. Drug Deliv. Rev. 156 (2020) 4–22, https://doi.org/10.1016/j.addr.2020.06.022.
[56] L. Román-Álamo, M. Allaw, Y. Avalos-Padilla, M.L. Manca, M. Manconi, F. Fulgheri, J. Fernández-Lajo, L. Rivas, J.A. Vázquez, J.E. Peris, X. Roca-Geronès, S. Poonlaphdecha, M.M. Alcover, R. Fisa, C. Riera, X. Fernàndez-Busquets, In vitro evaluation of aerosol therapy with pentamidine-loaded liposomes coated with chondroitin sulfate or heparin for the treatment of leishmaniasis, Pharmaceutics 15 (2023) 1163, https://doi.org/10.3390/pharmaceutics15041163.
[57] M. Perra, M.L. Manca, C.I.G. Tuberoso, C. Caddeo, F. Marongiu, J.E. Peris, G. Orrù, A. Ibba, X. Fernàndez-Busquets, S. Fattouch, G. Bacchetta, M. Manconi, A green and cost-effective approach for the efficient conversion of grape byproducts into innovative delivery systems tailored to ensure intestinal protection and gut microbiota fortification, Innov. Food Sci. Emerg. Technol. 80 (2022) 103103, https://doi.org/10.1016/j.ifset.2022.103103.
[58] X. Nian, J. Zhang, S. Huang, K. Duan, X. Li, X. Yang, Development of nasal vaccines and the associated challenges, Pharmaceutics 14 (2022) 1983, https://doi.org/10.3390/pharmaceutics14101983.
[59] European Medicines Agency, Guideline on the Pharmaceutical Quality of Inhalation and Nasal Products Draft, 2012, pp. 1–15.
[60] V. US Food Kulkarni, C. and D.A. Shaw, Guidance for Industry Nasal Spray and Inhalation Solution, Suspension, and Spray Drug Products — Chemistry, Manufacturing, and Controls Documentation, U.S. Department of Health and Human Services Food and Drug Administration Center for Drug Evaluation an, Online, 2002, pp. 10–15. https://www.fda.gov/media/70857/download.
[61] J.Z. Chen, W.H. Finlay, A. Martin, In vitro regional deposition of nasal sprays in an idealized nasal inlet: Comparison with in vivo gamma scintigraphy, Pharm. Res. 39 (2022) 3021–3028, https://doi.org/10.1007/s11095-022-03388-7.
[62] A. Maaz, I.S. Blagbrough, P.A. De Bank, In vitro evaluation of nasal aerosol depositions: an insight for direct nose to brain drug delivery, Pharmaceutics 13 (2021) 1079, https://doi.org/10.3390/pharmaceutics13071079.
[63] D.L. Swift, N. Montassier, P.K. Hopke, K. Karpen-Hayes, Y.S. Cheng, Yin Fong Su, Hsu Chi Yeh, J.C. Strong, Inspiratory deposition of ultrafine particles in human nasal replicate cast, J. Aerosol Sci. 23 (1992) 65–72, https://doi.org/10.1016/0021-8502(92)90318-P.
[64] H. Xu, R.F. Alzhrani, Z.N. Warnken, S.G. Thakkar, M. Zeng, H.D.C. Smyth, R. O. Williams, Z. Cui, Immunogenicity of Antigen adjuvanted with AS04 and its deposition in the upper respiratory tract after intranasal administration, Mol. Pharm. 17 (2020) 3259–3269, https://doi.org/10.1021/acs.molpharmaceut.0c00372.

[65] Z. Teng, L.Y. Meng, J.K. Yang, Z. He, X.G. Chen, Y. Liu, Bridging nanoplatform and vaccine delivery, a landscape of strategy to enhance nasal immunity, J. Contr. Release 351 (2022) 456–475, https://doi.org/10.1016/j.jconrel.2022.09.044.
[66] R. Pabst, Mucosal vaccination by the intranasal route. Nose-associated lymphoid tissue (NALT)-Structure, function and species differences, Vaccine 33 (2015) 4406–4413, https://doi.org/10.1016/j.vaccine.2015.07.022.
[67] Y. Ma, Y. Zhuang, X. Xie, C. Wang, F. Wang, D. Zhou, J. Zeng, L. Cai, The role of surface charge density in cationic liposome-promoted dendritic cell maturation and vaccine-induced immune responses, Nanoscale 3 (2011) 2307–2314, https://doi.org/10.1039/c1nr10166h.
[68] A.R. Nikpoor, M.R. Jaafari, P. Zamani, M. Teymouri, H. Gouklani, E. Saburi, S. A. Darban, A. Badiee, A. Bahramifar, M. Fasihi-Ramandi, R.A. Taheri, Cell cytotoxicity, immunostimulatory and antitumor effects of lipid content of liposomal delivery platforms in cancer immunotherapies. A comprehensive in-vivo and in-vitro study, Int. J. Pharm. 567 (2019) 118492, https://doi.org/10.1016/j.ijpharm.2019.118492.
[69] E.R. Sherwood, T. Toliver-Kinsky, Mechanisms of the inflammatory response, Best Pract. Res. Clin. Anaesthesiol. 18 (2004) 385–405, https://doi.org/10.1016/j.bpa.2003.12.002.
[70] A. Mantovani, A. Ponzetta, A. Inforzato, S. Jaillon, Innate immunity, inflammation and tumour progression: double-edged swords, J. Intern. Med. 285 (2019) 524–532, https://doi.org/10.1111/joim.12886.
[71] J. Korbecki, K. Bajdak-Rusinek, The effect of palmitic acid on inflammatory response in macrophages: an overview of molecular mechanisms, Inflamm. Res. 68 (2019) 915–932, https://doi.org/10.1007/s00011-019-01273-5.
[72] H. Wajant, D. Siegmund, TNFR1 and TNFR2 in the control of the life and death balance of macrophages, Front. Cell Dev. Biol. 7 (2019) 91, https://doi.org/10.3389/fcell.2019.00091.
[73] H.C. Bygd, L. Ma, K.M. Bratlie, Physicochemical properties of liposomal modifiers that shift macrophage phenotype, Mater. Sci. Eng. C 79 (2017) 237–244, https://doi.org/10.1016/j.msec.2017.05.032.
[74] Y. Cruz-Leal, M.F. Lucatelli Laurindo, L. Osugui, M. del C. Luzardo, A. López-Requena, M.E. Alonso, C. Álvarez, A.F. Popi, M. Mariano, R. Pérez, M.E. Lanio, Liposomes of phosphatidylcholine and cholesterol induce an M2-like macrophage phenotype reprogrammable to M1 pattern with the involvement of B-1 cells, Immunobiology 219 (2014) 403–415, https://doi.org/10.1016/j.imbio.2014.01.006.